

Supplementary Materials for

Cascade-responsive size/charge bidirectional-tunable nanodelivery penetrates pancreatic tumor barriers

*Yiqi Shi,^a Jinghan Liao,^b Cuiyun Zhang,^a Qi Wu,^a Shanshan Hu,^a Ting Yang,^c Jihong Liu,^a Zhirong Zhu,^a Qi Wang,^{*a} and Wei-Hong Zhu^a*

Y. Shi and J. Liao contributed equally.

^a Shanghai Key Laboratory of Functional Materials Chemistry, Key Laboratory for Advanced Materials and Institute of Fine Chemicals, Joint International Research Laboratory of Precision Chemistry and Molecular Engineering, Feringa Nobel Prize Scientist Joint Research Center, Frontiers Science Center for Materiobiology and Dynamic Chemistry, School of Chemistry and Molecular Engineering, East China University of Science and Technology, Shanghai 200237, China.

^b State Key Laboratory of Systems Medicine for Cancer, Shanghai Cancer Institute, Reni Hospital, School of Medicine, Shanghai Jiao Tong University, 2200/25 Xietu Road, Shanghai, 200032, China.

^c Guangdong Key Laboratory of Nanomedicine, CAS-HK Joint Lab for Biomaterials, Shenzhen Institutes of Advanced Technology, Chinese Academy of Sciences, Shenzhen, 518055, China.

This PDF file includes:

Figs. S1 to S33
Movies S1 to S5

Other Supplementary Materials for this manuscript include the following:

Movies S1 to S5

Table of Contents

1 Experimental Section	3
1.1 Materials and characterization	3
1.2 Synthesis of TK-COOH.....	3
1.3 Synthesis of Cz-T-CHO.....	3
1.4 Synthesis of TCM-Cz	3
1.5 Synthesis of TCM-Cz-OH	4
1.6 Synthesis of TCM	4
1.7 Synthesis of TCM-TK-PEI	4
1.8 Total ROS detection	5
1.9 Preparation and characterization of G/R@TKP/HA	5
1.10 In vitro HAase-responsive size and charge tuning assay.....	5
1.11 In vitro HAase/ROS-cascade responsive size and charge tuning assay	5
1.12 Cell lines and culture condition	6
1.13 Multicellular tumor spheroids imaging	6
1.14 Cellular uptake behavior	6
1.15 Lysosome escape assay.....	6
1.16 Intracellular ROS detection	7
1.17 Lysosomal membrane damage	7
1.18 Cytotoxicity studies	7
1.19 In vitro antitumor efficacy evaluation	7
1.20 Live/dead cell staining.....	8
1.21 JC-1 assay of mitochondrial membrane potential	8
1.22 In vivo fluorescence imaging.....	8
1.23 In vivo microscopy imaging	8
1.24 In vivo antitumor efficacy evaluation.....	9
1.25 Statistical analysis.....	9
2 Supporting Figures	10
3 Characterization of Compounds	30
4 Supporting Movies	43

1 Experimental Section

1.1 Materials and characterization

All solvents and chemicals, unless special stated, were purchased commercially in analytical grade and used without further purification. KRAS siRNA was purchased from RiboBio (Guangzhou, China). ^1H and ^{13}C NMR spectra in deuterium generation were obtained with a Bruker AvanceIII 400 MHz NMR spectrometer at room temperature using TMS as an internal standard. High resolution mass spectrometry (HRMS) spectra were measured with a Waters LCT Premier XE spectrometer. UV-Vis absorption and fluorescence spectra were recorded on an Agilent Cary 60 spectrophotometer and Varian Cary Eclipse fluorescence spectrophotometer (10 × 10 mm quartz cuvette), respectively. Infrared spectra were recorded on Fourier Transform-Infrared spectrometer. Dynamic light scattering (DLS) experiments were conducted with Zetasizer Nano-ZS (Malvern Instruments, Worcestershire, UK). Transmission electron microscope (TEM) images were captured by JEOL JEM-1400 and Hitachi H-9500 transmission electron microscope. Confocal fluorescence images were performed on Leica TCS SP8 laser scanning confocal microscopy. Cell cytotoxicity test results were recorded by Bio-Rad iMark microplate reader. In vivo fluorescence images were measured with PerkinElmer IVIS Spectrum. The real-time in vivo tumor penetrability and retention was monitored by the In Vivo Live Cell Imaging Platform (IVM-CMS, IVIM Technology, Korea).

1.2 Synthesis of TK-COOH

3-mercaptopropionic acid (10 g, 94.4 mmol), trifluoroacetic acid (40 μL) and acetone (3.32 mL, 2.6 g, 42.92 mmol) were added into a 100 mL single-mouth flask and stirred at room temperature for 4 h to produce white solid. The white solid was filtered, washed with n-hexane and ice water in turn, and vacuum dried to obtain TK-COOH (10.2 g, yield 90%). ^1H NMR (400 MHz, CDCl_3 , ppm): δ 2.90 (d, $J = 7.4$ Hz, 4H, $-\text{SCH}_2\text{CH}_2\text{CO}$), 2.68 (t, $J = 7.4$ Hz, 4H, $-\text{SCH}_2\text{CH}_2\text{CO}$), 1.60 (s, 6H, $-\text{CH}_3$). High-resolution mass spectrometry (ESI positive ion mode for $[\text{M} - \text{H}]^-$): Calcd. For $\text{C}_9\text{H}_{15}\text{O}_4\text{S}_2$: 251.0406; found: 251.0408.

1.3 Synthesis of Cz-T-CHO

In nitrogen atmosphere, N, N-dimethylformamide (DMF) (40 mL), carbazole (5 g, 30 mmol) and 5-bromo-2-thiophenecarboxaldehyde (7.14 g, 37.4 mmol) were added into three neck flask and stirred at room temperature for 30 min. Copper (I) iodide (CuI) (0.95 g, 5 mmol) and potassium carbonate (K_2CO_3) (6.2 g, 44.9 mmol) were added to the flask and then the mixture was reacted at 140°C for 48 h. At the end of the reaction, the insoluble matter was removed by filtration. The solvent was then removed under reduced pressure, and the crude product was purified by silica gel column chromatography (PE/EA, v/v, 15/1) to obtain the light yellow solid, Cz-T-CHO (5.60g, yield 68%). ^1H NMR (400 MHz, CDCl_3 , ppm): δ 9.96 (s, 1H, $-\text{CHO}$), 8.11 (dt, $J = 7.7, 1.0$ Hz, 2H, Ar-H), 7.89 (d, $J = 4.1$ Hz, 1H, thiophene-H), 7.78 – 7.65 (m, 2H, Ar-H), 7.48 (ddd, $J = 8.3, 7.2, 1.3$ Hz, 2H, Ar-H), 7.40 – 7.33 (m, 3H, Ar-H). High-resolution mass spectrometry (ESI positive ion mode for $[\text{M} + \text{H}]^+$): Calcd. For $\text{C}_{17}\text{H}_{12}\text{NOS}$: 278.0634; found: 278.0631.

1.4 Synthesis of TCM-Cz

TCM-1 (590 mg, 1.57 mmol), Cz-T-CHO (146 mg, 0.53 mmol), and acetonitrile (10 mL) were successively added into the dry 50 mL double-mouth flask. After stirring well, piperidine (0.12 mL) was added into the flask. In nitrogen atmosphere, the mixture was reacted at 95°C for 12 h. Then, the reaction was cooled to room temperature and the solvent was removed under reduced

pressure. The crude product was purified by silica gel column chromatography (PE/DCM, v/v, 1/4) to obtain the dark red solid, TCM-Cz (134 mg, yield 40%). ¹H NMR (400 MHz, DMSO-*d*₆, ppm): δ 8.22 (dt, *J* = 7.8, 1.0 Hz, 2H, Ar-H), 7.73 – 7.56 (m, 8H, Ar-H), 7.55 – 7.30 (m, 10H, Ar-H), 7.20 (d, *J* = 2.3 Hz, 1H, Ar-H), 7.03 (s, 2H, alkene-H), 5.87 (d, *J* = 15.8 Hz, 1H, alkene-H), 2.14 (s, 3H, -CH₃). High-resolution mass spectrometry (ESI positive ion mode for [M + Na]⁺): Calcd. For C₄₂H₂₇N₅NaS: 656.1879; found: 656.1882.

1.5 Synthesis of TCM-Cz-OH

TCM-Cz (100 mg, 0.16 mmol), 4-hydroxy benzaldehyde (385 mg, 3.16 mmol), and acetonitrile (10 mL) were added successively to a dry 50 mL double-mouth flask. After stirring well, piperidine (0.25 mL) was added into the flask. In nitrogen atmosphere, the mixture was reacted at 95°C for 12 h. Then, the reaction was cooled to room temperature and the solvent was removed under reduced pressure. The crude product was purified by silica gel column chromatography (DCM/MeOH, v/v, 99/1) to obtain the red solid, TCM-Cz-OH (25 mg, yield 21.5%). ¹H NMR (400 MHz, DMSO-*d*₆, ppm): δ 10.04 (s, 1H, Ph-OH), 8.23 (d, *J* = 7.8 Hz, 2H, Ar-H), 7.74 – 7.61 (m, 8H, Ar-H), 7.53 – 7.28 (m, 12H, Ar-H), 7.10 (d, *J* = 8.4 Hz, 3H, Ar-H), 6.83 (d, *J* = 16.0 Hz, 1H, alkene-H), 6.73 (d, *J* = 8.5 Hz, 2H, Ar-H), 6.04 (d, *J* = 15.9 Hz, 1H, alkene-H), 5.97 (d, *J* = 15.8 Hz, 1H, alkene-H). High-resolution mass spectrometry (ESI positive ion mode for [M - H]⁻): Calcd. For C₄₉H₃₀N₅O₅S: 736.2166; found: 736.2162.

1.6 Synthesis of TCM

TK-COOH (47.4 mg, 0.188 mmol) was added to acetic anhydride (0.2 mL). In nitrogen atmosphere, the mixture was stirred at room temperature for 2 h. At the end of the reaction, toluene (1 mL) was added to the reaction system and the solvent was removed under reduced pressure, and the process was repeated three times. The oil product was dissolved in anhydrous dichloromethane (1 mL), and TCM-Cz-OH (46.2 mg, 0.063 mmol) and catalytic DMAP (0.5 mg, 0.004 mmol) were added. In nitrogen atmosphere, the mixture was stirred at room temperature for 24 h. Then, the solvent was removed under reduced pressure. The crude product was purified by silica gel column chromatography (DCM/MeOH, v/v, 40/1) to obtain the dark red solid, TCM (28.6 mg, yield 47%). ¹H NMR (400 MHz, DMSO-*d*₆, ppm): δ 8.25 – 8.21 (m, 2H, Ar-H), 7.75 – 7.59 (m, 8H, Ar-H), 7.55 – 7.45 (m, 7H, Ar-H), 7.44 – 7.38 (m, 2H, Ar-H), 7.37 – 7.29 (m, 5H, Ar-H), 7.12 (dd, *J* = 10.3, 3.4 Hz, 3H, Ar-H), 6.94 (s, 1H, alkene-H), 6.29 (d, *J* = 16.0 Hz, 1H, alkene-H), 5.98 (d, *J* = 15.7 Hz, 1H, alkene-H), 2.87 (d, *J* = 3.7 Hz, 4H, -SCH₂CH₂COOPh), 2.74 (d, *J* = 7.1 Hz, 4H, -CH₂CH₂COOH), 1.55 (s, 6H, -CH₃). ¹³C NMR (151 MHz, DMSO-*d*₆, ppm): δ 190.99, 173.12, 171.94, 166.19, 163.49, 159.80, 152.26, 149.40, 148.16, 140.60, 139.65, 138.81, 137.68, 137.34, 136.47, 132.17, 131.47, 131.15, 130.96, 130.89, 130.66, 130.45, 129.51, 128.80, 128.45, 127.91, 126.87, 126.29, 125.71, 123.20, 121.36, 120.71, 118.34, 116.56, 116.10, 115.93, 115.51, 115.04, 51.56, 34.31, 33.89, 33.24, 30.65, 25.08. High-resolution mass spectrometry (ESI positive ion mode for [M - H]⁻): Calcd. For C₅₈H₄₄N₅O₄S₃: 970.2550; found: 970.2538.

1.7 Synthesis of TCM-TK-PEI

TCM (20 mg, 0.0206 mmol) and NHS (2.9 mg, 0.0251 mmol) were dissolved in anhydrous tetrahydrofuran (0.5 mL) and stirred in dry nitrogen atmosphere. Then, 0.5 mL EDC (4.0 mg, 0.0253 mmol) of anhydrous THF solution was injected into the system at 0°C. Continue stirring at room temperature for 24 h. After the reaction, the filtrate was filtered and rotary-dried dry to obtain the active intermediate. PEI was dissolved in anhydrous DMSO (1.0 mL). The active intermediate

was dissolved in anhydrous DCM (0.5mL) and then added to PEI solution slowly. After finishing adding, DCM was removed under reduced pressure. Then the reaction solution was stirred at room temperature for 48 h in dry nitrogen atmosphere. At the reaction, the mixture was dialyzed (MWCO 10000 Da) against deionized water for three days. The polymer TCM-TK-PEI was obtained as yellow viscous gel after freeze drying.

1.8 Total ROS detection

A reactive oxygen species (ROS)-sensitive indicator, dichlorofluorescein diacetate (DCFH-DA), was used to detect the ROS production upon light irradiation. DCFH-DA (2 mL, 1mM in ethanol) were reacted with NaOH aqueous solution (8 mL, 10 mM) for 30 min at room temperature, and neutralized the hydrolysate with 40 mL PBS buffer solution to obtain the stock solution with a concentration of 40 μ M. The total ROS production of TCM-TK-PEI (0.15 mg/mL) and TCM (10 μ M) under white light irradiation (80 mW cm⁻²) was tested using DCFH-DA (40 μ M) as an indicator. After the white light irradiation, the fluorescence change in the solution was measured upon excitation at 488 nm and the emission was collected from 500 to 600 nm. The fluorescence intensity at 525 nm was plotted against the irradiation time.

1.9 Preparation and characterization of G/R@TKP/HA

TCM-TK-PEI can self-assemble into nanoparticles in water, which is denoted as TKP. Self-assembly method was used to form TCM-TK-PEI@Gem (denoted as G@TKP). Briefly, 376 μ L 1.0 mg mL⁻¹ gemcitabine (Gem) solution was added to 5.0 mg TCM-TK-PEI. Then it was sonicated with an ultrasonic cell grinder for 10 min, followed by magnetic stirring for 1 hour to prepare G@TKP. Subsequently, G@TKP and KRAS siRNA were mixed at 2.5/1 (TCM-TK-PEI/siRNA, w/w) weight ratio, vortexed and then incubated for 1 h at 37°C to form TCM-TK-PEI@Gem/KRAS siRNA complex (denoted as G/R@TKP). Finally, G/R@TKP was added to hyaluronic acid (HA) at 1/1 (TCM-TK-PEI/HA, w/w) weight ratio and the mixture was stirred gently for 1 h at room temperature to obtain TCM-TK-PEI@Gem/siRNA/HA complex (denoted as G/R@TKP/HA). DLS was adopted to characterize the size and zeta potential of TKP, G@TKP, G/R@TKP, and G/R@TKP/HA. The morphology of G/R@TKP/HA was observed by TEM. And the particle size alteration and polydisperse index (PDI) of G/R@TKP/HA was monitored to explore the stability of G/R@TKP/HA. The siRNA condensation of G/R@TKP/HA was qualitatively explored by using the gel retardation assay (1% agarose gel).

1.10 In vitro HAase-responsive size and charge tuning assay

G/R@TKP/HA was incubated with hyaluronidase (HAase) at 37°C. And then the particle size and zeta potential of the mixture were examined using DLS. The morphology of G/R@TKP/HA treated with HAase was examined using TEM.

1.11 In vitro HAase/ROS-cascade responsive size and charge tuning assay

HAase/ROS dual-cascade response process of G/R@TKP/HA was simulated by sequentially adding HAase and ROS. We investigated ROS cascade response under light and non-light conditions, respectively. Under light condition, G/R@TKP/HA was initially incubated with hyaluronidase (HAase) at 37°C, and then exposed to white light irradiation (40 mW cm⁻², 8 min). Under non-light condition, G/R@TKP/HA was incubated with HAase followed by the addition of H₂O₂. The diameter and zeta potential of G/R@TKP/HA after HAase treatment followed by ROS were examined using DLS, while the morphology was examined using TEM.

1.12 Cell lines and culture condition

Human Pancreatic Carcinoma (PANC1) Cells were provided by the Shanghai Cancer Institute. Cells were propagated in cell culture flask at 37°C under humidified 5% CO₂ atmosphere. Dulbecco's modified eagle medium (DMEM, GIBCO/Invitrogen, Camarillo, CA, USA) was supplemented with 1% penicillin-streptomycin (10,000 U mL⁻¹ penicillin, and 10 mg mL⁻¹ streptomycin, Solarbio life science, Beijing, China) and 10% fetal bovine serum (FBS, Biological Industry, Kibbutz Beit Haemek, Israel).

1.13 Multicellular tumor spheroids imaging

PANC1 cells were seeded at a density of 6×10^3 cells/well into multiple 96-well plates previously coated with agarose, supplemented with 50 μ L fresh medium every 48 h, and cultured for 1 weeks at 37°C and 5% CO₂ atmosphere. The spheroids were incubated with G/R@TKP/HA or G/R@TKP (the concentration of TCM-TK-PEI: 0.05 mg/mL) at 37°C and 5% CO₂ atmosphere for 4 h in the dark. Then the culture medium was removed, and the spheroids were washed with PBS. Fluorescence images were captured with CLSM in each 5 μ m layer of spheroids by scanning along the z-axis. The TCM fluorescence signal at 550-700 nm was collected at the excitation wavelength of 461 nm.

1.14 Cellular uptake behavior

PANC1 cells were seeded onto glass-bottom cell culture dishes (Φ 20 mm, NEST) at a density of 1×10^5 cells/well and allowed to adhere for 12 h. The cells were incubated with G/R@TKP/HA or G/R@TKP (the concentration of TCM-TK-PEI: 0.05 mg/mL) at 37°C and 5% CO₂ atmosphere for 15 min, 30 min and 1 h. Then the culture medium was removed, and the cells were washed three times with PBS. Finally, 1 mL of PBS was added, followed by cell imaging with CLSM (Leica TCS SP8). The AIE fluorescence signal of TCM at 550-700 nm was collected at the excitation wavelength of 461 nm. For the HA competitive inhibition experiment, PANC1 cells were pre-treated with HA (10 mg/mL) for 2 h to block the CD44 receptor. After washing with PBS twice, the cells were incubated with G/R@TKP/HA or G/R@TKP for 1 h. Then the culture medium was removed, and the cells were washed three times with PBS. Finally, cell imaging was captured with CLSM. The TCM fluorescence signal at 550-700 nm was collected at the excitation wavelength of 461 nm. For gene drug delivery efficiency experiment, the cells were incubated with Free drug (Gem + Cy5-labeled siRNA) or G/R@TKP/HA encapsulating Cy5-siRNA at 37°C and 5% CO₂ atmosphere for 1 h. Then the culture medium was removed, and the cells were washed three times with PBS, followed by 1 mL of PBS was added. Finally, cell imaging was captured with CLSM by collecting Cy5 fluorescence signal.

1.15 Lysosome escape assay

PANC1 cells were seeded onto glass-bottom cell culture dishes (Φ 20 mm, NEST) at a density of 1×10^5 cells/well and allowed to adhere for 12 h. The cells were incubated with G/R@TKP/HA (the concentration of TCM-TK-PEI: 0.05 mg/mL) for 1 h. Then, the culture was removed and the cells were washed three times with PBS. Fresh medium without G/R@TKP/HA was added to the cells and the cells were incubated for additional 0, 1 and 3 h. After removing culture and washing with PBS twice, LysoTracker Red (50 nM) and Hoechst 33342 were used to stain lysosome and nucleus respectively. Cell imaging was captured with CLSM. For the light group, the cells were exposed to the white light (40 mW cm⁻²) for 8 min after replacing fresh medium.

1.16 Intracellular ROS detection

The intracellular ROS production of TCM-TK-PEI/HA (denoted as TKP/HA) upon white light irradiation was detected using DCFH-DA as the indicator. None fluorescent DCFH-DA can be oxidized by ROS to produce fluorescent dichlorofluorescein (DCFH). PANC1 cells were seeded onto glass-bottom cell culture dishes (Φ 20 mm, NEST) at a density of 1×10^5 cells/well and allowed to adhere for 12 h. The cells were incubated with TKP/HA (the concentration of TCM-TK-PEI: 0.05 mg/mL) for 1 h. After removing culture and washing with PBS for three times, the cells were incubated with DCFH-DA (10 μ M) for 30 min. Then, the culture was removed and the cells were washed with PBS. After white light irradiation (40 mW cm^{-2}) for 5 min or in the dark, cell imaging was captured with CLSM. The fluorescence signal at 505-560 nm was collected at the excitation wavelength of 488 nm.

1.17 Lysosomal membrane damage

The lysosomal membrane damage was detected by acridine orange (AO). AO exhibits green fluorescence within cytoplasm and nuclei, while emitting red fluorescence in acidic organelles like endo/lysosomes. PANC1 cells were seeded onto glass-bottom cell culture dishes (Φ 20 mm, NEST) at a density of 1×10^5 cells/well and allowed to adhere for 12 h. The cells were incubated with G/R@TKP/HA (the concentration of TCM-TK-PEI: 0.05 mg/mL) for 1 h. Then, the culture was removed and the cells were washed three times with PBS. The cells were stained with AO. Then, the culture was removed and the cells were washed with PBS. Cell imaging was captured with CLSM. The excitation was 488 nm, and the emission filter was 505-525 nm (green channel) and 610-640 nm (red channel). For the light group, the cells were exposed to the white light (40 mW cm^{-2}) for 8 min before AO staining.

1.18 Cytotoxicity studies

The viabilities of PANC1 cells were obtained by MTT (3-(4, 5-dimethylthiazol-2-yl) -2,5-diphenyltetrazolium bromide) assay. Briefly, PANC1 cells were seeded onto 96-well plates at a density of 1×10^4 cells/well and cultured for 12 h. After the cells were attached to the wall, the cells were incubated with various concentration of TKP/HA or TCM-TK-PEI (denoted as TKP) (the concentration of TCM-TK-PEI: 0, 5, 10, 25, 50, 75, 100 μ g/mL) for 1 h, then replaced the TKP/HA or T solution with fresh DMEM. After culturing in the dark for 24 h, 10 μ L MTT solution (5 mg/mL) was added to each well and further cultured in the dark for 4 h. Carefully removing the liquid supernatant, 100 μ L DMSO was added to each well to dissolve the crystals. The UV absorbance of each well was measured by a microplate reader (Bio Tek Synergy H4) at 570 nm.

1.19 In vitro antitumor efficacy evaluation

In vitro antitumor efficacy was evaluated by MTT assay. Briefly, PANC1 cells were seeded onto 96-well plates at a density of 1×10^4 cells/well and cultured for 12 h. After the cells were attached to the wall, the cells were incubated with various concentration of Gem + KRAS siRNA (denoted as Free drugs), TKP/HA or G/R@TKP/HA (the concentration of TCM-TK-PEI: 0, 5, 25, 50 μ g/mL) for 1 h, then replaced the Free drugs, TKP/HA or G/R@TKP/HA solution with fresh DMEM. After culturing in the dark for 24 h, 10 μ L MTT solution (5 mg/mL) was added to each well and further cultured in the dark for 4 h. Carefully removing the liquid supernatant, 100 μ L DMSO was added to each well to dissolve the crystals. The UV absorbance of each well was measured by a microplate reader (Bio Tek Synergy H4) at 570 nm. The relative cell viability was

calculated based on the following formula. For the light group, the cells were exposed to the white light (40 mW cm^{-2}) for 15 min after replacing TKP/HA or G/R@TKP/HA solution with fresh DMEM, and the following procedures were the same as above.

1.20 Live/dead cell staining

PANC1 cells were seeded onto glass-bottom cell culture dishes (Φ 20 mm, NEST) at a density of 1×10^5 cells/well and allowed to adhere for 12 h. The cells were incubated with Free drugs, G/R@TKP/HA or TKP/HA (the concentration of TCM-TK-PEI: 0.05 mg/mL) for 1 h. After removing culture and washing with PBS, the cells were incubated with fresh DMEM for 12 h. Then, the cells were stained with Calcein-AM/PI mixtures ($1 \mu\text{mol L}^{-1}$ Calcein-AM, 1 mg mL^{-1} PI) for 30 min. Cell imaging was captured with CLSM. Green channel from Calcein-AM: $\lambda_{\text{ex}} = 496 \text{ nm}$, $\lambda_{\text{em}} = 500\text{-}540 \text{ nm}$, red channel from PI: $\lambda_{\text{ex}} = 561 \text{ nm}$, $\lambda_{\text{em}} = 590\text{-}650 \text{ nm}$. For the light group, the cells were exposed to the white light (40 mW cm^{-2}) for 15 min after replacing the fresh medium, and the following procedures were the same as above.

1.21 JC-1 assay of mitochondrial membrane potential

Cell apoptosis was assessed using JC-1 as an indicator, monitoring mitochondrial membrane potential ($\Delta\Psi\text{m}$). JC-1 exists in aggregate form emitting red fluorescence around 590 nm in normal cells due to high $\Delta\Psi\text{m}$, while during cell apoptosis, it switches to monomer form emitting green fluorescence at 529 nm owing to a decline in $\Delta\Psi\text{m}$. Leveraging the ratio of green to red fluorescence, cell apoptosis can be detected. Carbonyl cyanide 3-chlorophenylhydrazone (CCCP), a typical mitochondrial disturber, served as the positive control. PANC1 cells were seeded onto glass-bottom cell culture dishes (Φ 20 mm, NEST) at a density of 1×10^5 cells/well and allowed to adhere for 12 h. The cells were incubated with Free drugs, G/R@TKP/HA or TKP/HA (the concentration of TCM-TK-PEI: 0.05 mg/mL) for 1 h. After removing culture and washing with PBS, the cells were incubated with fresh DMEM for 12 h. Then, the culture was replaced by 0.5 mL fresh DMEM and 0.5 mL JC-1 operating fluid with sufficient mixing. The cells were incubated for 20 min. Subsequently, the culture was removed and the cells were washed with JC-1 staining buffer ($1\times$) for two times. Cell imaging was captured with CLSM. The fluorescence signal of monomeric form of JC-1 at 500-550 nm was collected at the excitation wavelength of 488 nm. The fluorescence signal of aggregated form of JC-1 at 570-620 nm was collected at the excitation wavelength of 543 nm. For the light group, the cells were exposed to the white light (40 mW cm^{-2}) for 15 min after replacing the fresh medium, and the following procedures were the same as above.

1.22 In vivo fluorescence imaging

G/R@TKP/HA or G/R@TKP (4 mg/kg TCM-TK-PEI) were injected to the PANC1 tumor-bearing mice through i.v. injection. Biodistribution images were collected by IVIS ($\lambda_{\text{ex}} = 461 \text{ nm}$, $\lambda_{\text{em}} = 550\text{-}700 \text{ nm}$) at various time points (0, 1, 3, 5, 8 h). PANC1 tumor-bearing mice were sacrificed at 8 h after the injection of G/R@TKP/HA or G/R@TKP. Ex vivo imaging of organs including heart, liver, spleen, lung, kidney and tumor was captured by IVIS.

1.23 In vivo microscopy imaging

The PANC1 tumor-bearing BALB/c nude mouse was intravenously injected with G/R@TKP/HA and Evans Blue (EB), respectively. After anesthesia, the mouse was exposed to subcutaneous tumor tissue and fixed under a microscope. The intravital microscopy images were captured by the

In Vivo Live Cell Imaging Platform (IVM-CMS, IVIM Technology, Korea). With the excitation wavelength of 488/640 nm, the G/R@TKP/HA/EB of fluorescence signal was collected at 500-550/663-733 nm.

1.24 In vivo antitumor efficacy evaluation

The BALB/c subcutaneous transplantation tumor models were established by injecting the flanks of the mice with 5×10^6 PANC1 cells. BALB/c mice bearing 100 mm³ tumors were divided into four groups randomly, PBS, Free Gem and KRAS siRNAs (Free drugs), G/R@TKP/HA and G/R@TKP/HA with white light (G/R@TKP/HA + L), respectively. The dose of Gem and KRAS siRNA was 0.8 mg kg⁻¹ and 0.09 mg kg⁻¹, respectively. And the concentration of various group was applied for subsequent animal experiments except for the PBS group. The mice were injected through i.v. injection every three days, and the weight and volume of the mice were measured and recorded every 3 days. The volume of the tumor was determined according to the equation $V = ab^2 \times 1/2$, where a and b were the longest and shortest diameters of the tumors. After 12 days of treatment, the tumors and organs were harvested, weighed, and imaged after the mice were euthanized. The tumors were washed with PBS three times, fixed with 10% neutral buffered formalin solution, embedded in paraffin, and cut into sections. H&E, TUNEL, Ki67, and CD44 staining were used to histopathologically analyze the tumor sections under a light microscope. Finally, H&E staining was also conducted for various important organs, including the heart, liver, spleen, lung, and kidney.

1.25 Statistical analysis

All statistical analyses were performed by using Origin version 2021. Data were reported as the mean \pm SD. The experimental data were statistically analyzed by using T-test with Origin version 2021. $P < 0.05$ was considered statistically significant (ns: $P > 0.05$, $0.01 < *P < 0.05$, $0.001 < **P < 0.01$, $0.0001 < ***P < 0.001$, $0.00001 < ****P < 0.0001$).

2 Supporting Figures

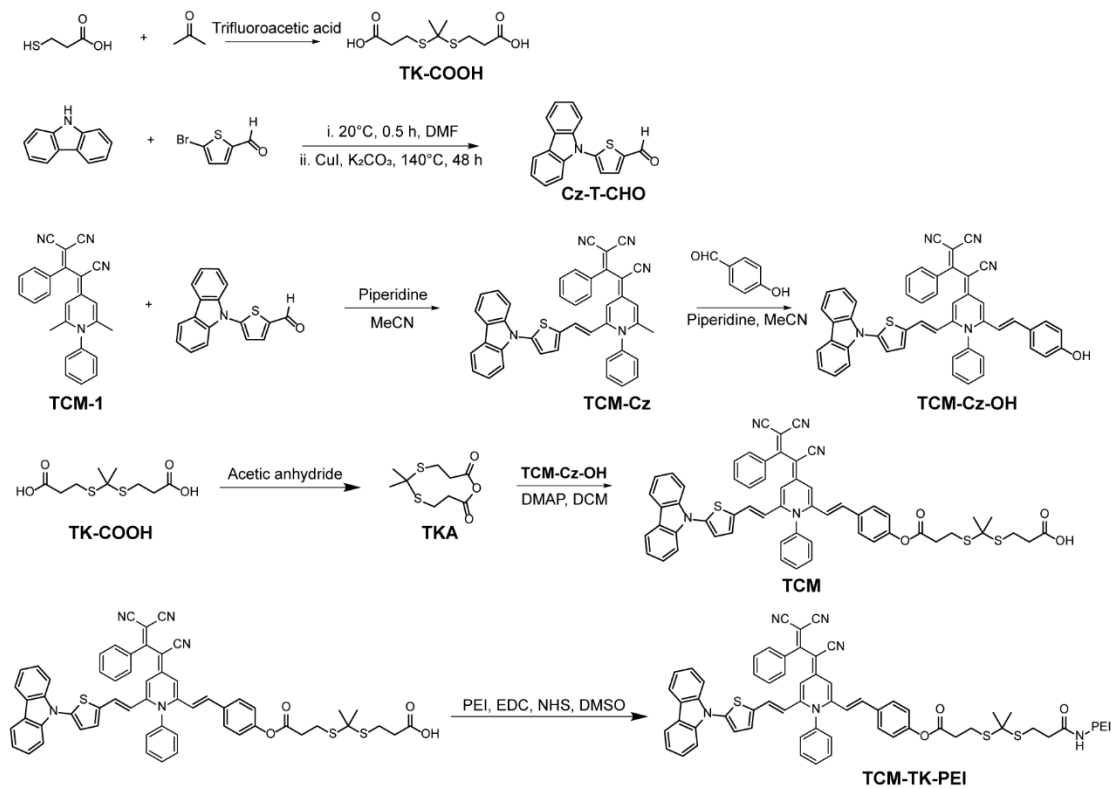


Fig. S1.
Synthesis of ROS-responsive polymer TCM-TK-PEI.

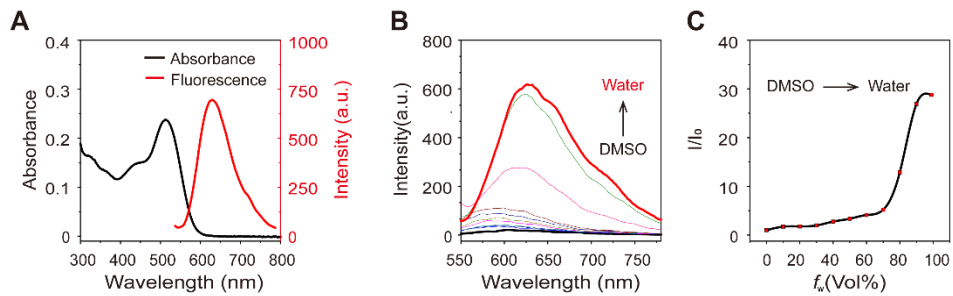


Fig. S2.

(A) Absorption and fluorescence spectra of TCM (10 μm) in 99% water, $\lambda_{\text{ex}} = 512$ nm. (B) Fluorescence spectra of TCM (10 μm) with different water fractions (f_w) in DMSO, $\lambda_{\text{ex}} = 512$ nm. (C) I/I_0 plot of TCM.

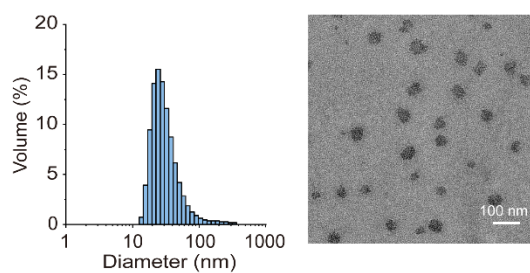


Fig. S3.

(A) Size distribution (left) and TEM image (right) of the nanoparticles self-assembled by TCM-TK-PEI.

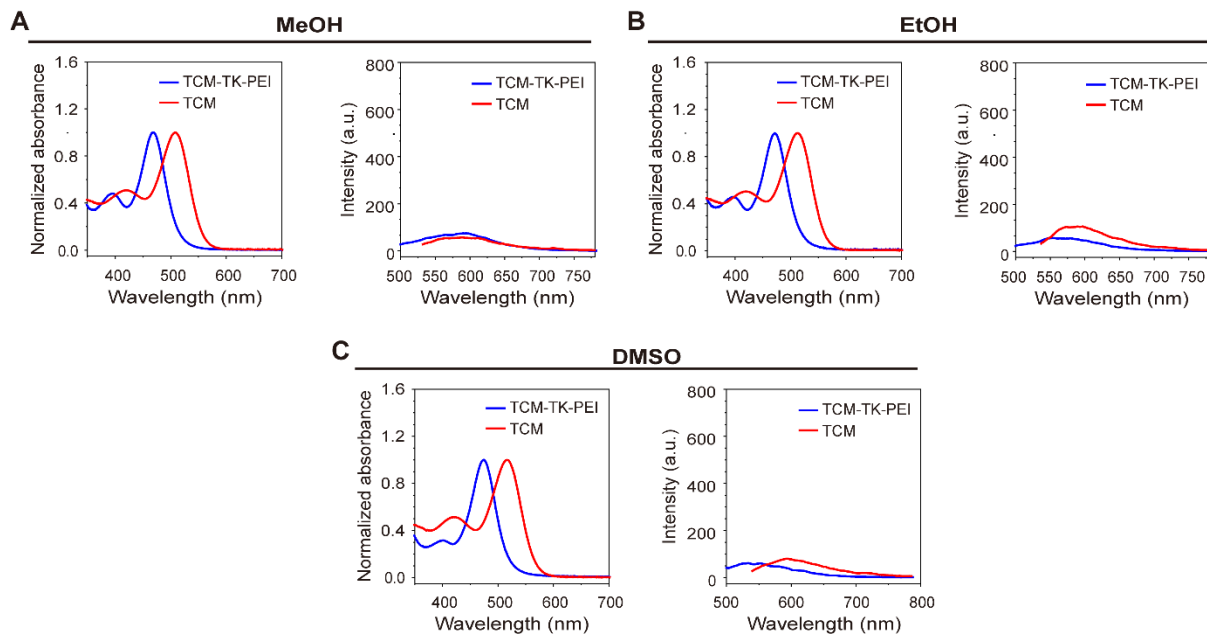


Fig. S4.

(A) Normalized absorption and fluorescence spectra of TCM and TCM-TK-PEI in MeOH, $\lambda_{\text{ex}} = \lambda_{\text{abs}}$. (B) Normalized absorption and fluorescence spectra of TCM and TCM-TK-PEI in EtOH, $\lambda_{\text{ex}} = \lambda_{\text{abs}}$. (C) Normalized absorption and fluorescence spectra of TCM and TCM-TK-PEI in DMSO, $\lambda_{\text{ex}} = \lambda_{\text{abs}}$.

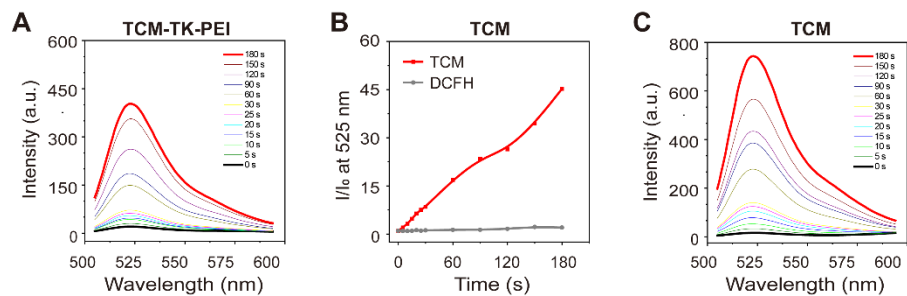


Fig. S5.

(A) Total ROS generation by TCM-TK-PEI (0.15 mg/mL) upon white light irradiation (40 mW cm^{-2}) using DCFH-DA ($40 \mu\text{m}$) as an indicator, $\lambda_{\text{ex}} = 488 \text{ nm}$. (B, C) Total ROS generation by TCM ($10 \mu\text{m}$) upon white light irradiation (40 mW cm^{-2}) using DCFH-DA ($40 \mu\text{m}$) as an indicator, $\lambda_{\text{ex}} = 488 \text{ nm}$.

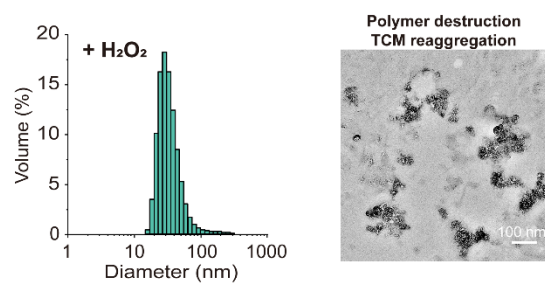


Fig. S6.

(A) Size distribution (left) and TEM image (right) of the nanoparticles self-assembled by TCM-TK-PEI after adding H₂O₂.

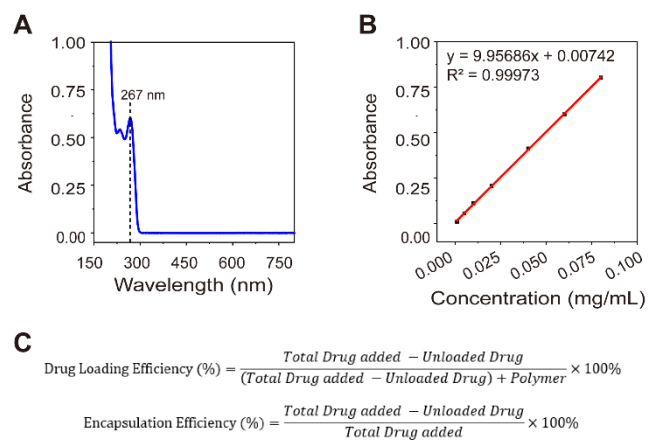


Fig. S7.

(A) Absorption spectrum of Gem in water. (B) Standard curve of Gem in water. (C) Calculation formula of drug loading efficiency and encapsulation efficiency.

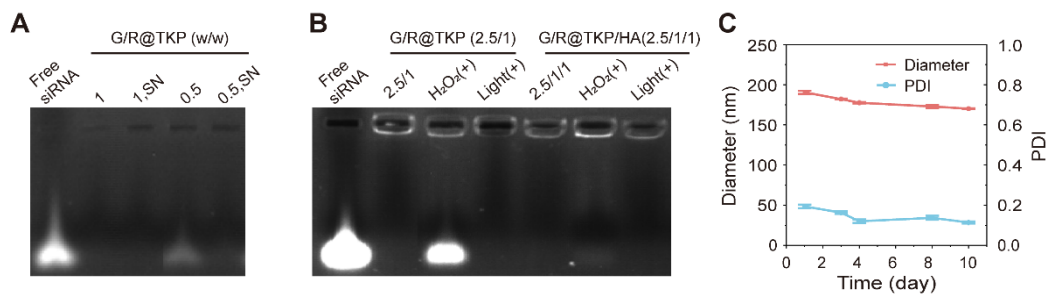


Fig. S8.

(A) Agarose gel electrophoresis assay of G/R@TKP at the different TCM-TK-PEI@Gem/siRNA weight ratios. The supernatant of G/R@TKP after centrifugation was denoted as SN. (B) Agarose gel electrophoresis assay of G/R@TKP (TCM-TK-PEI@Gem/siRNA weight ratio: 2.5/1) and G/R@TKP/HA (TCM-TK-PEI@Gem/siRNA/HA weight ratio: 2.5/1/1) in different conditions: with the addition of H₂O₂ denoted as H₂O₂(+), upon white light irradiation (40 mW cm⁻², 8 min) denoted as Light (+). (C) The particle size and PDI variation of G/R@TKP/HA over 10 days ($n = 3$).

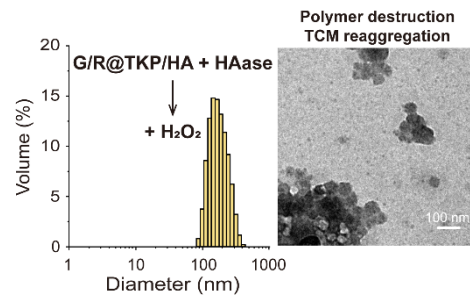


Fig. S9.

Size distribution (left) and TEM image (right) of the HAase/ROS-cascade response of G/R@TKP/HA after HAase treatment followed by adding H₂O₂.

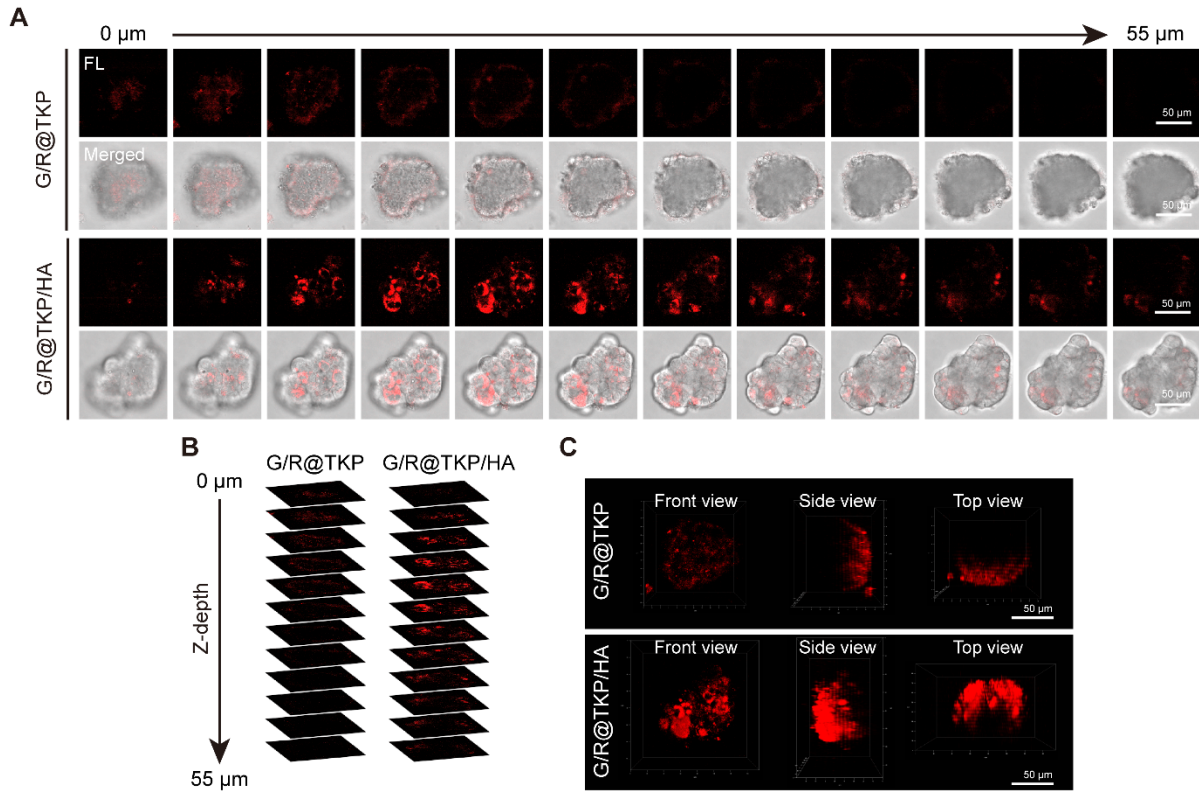


Fig. S10.

(A and B) Three-dimensional PANC1 MTs images obtained along the z-axis at different depths after treating with G/R@TKP or G/R@TKP/HA for 4 h. (C) Front, side and top views of three-dimensional reconstruction of PANC1 MTs in (A). All images share the same scale bar of 50 μm .

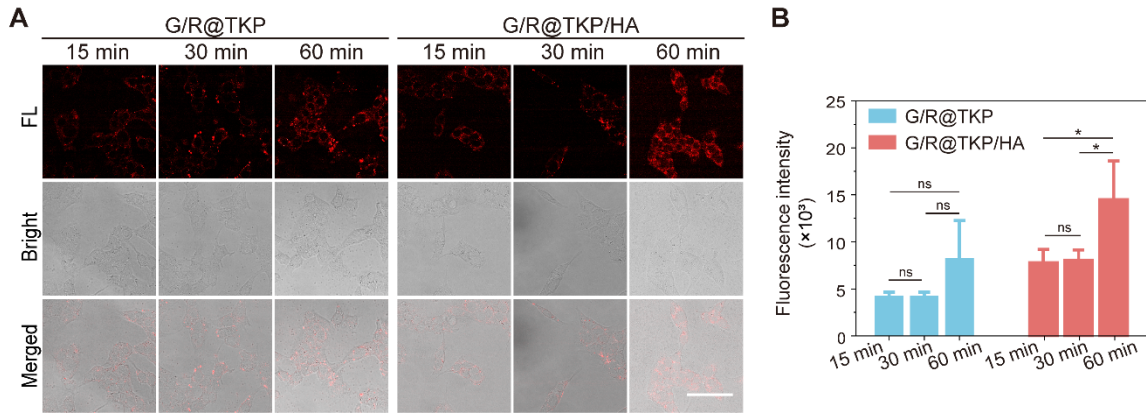


Fig. S11.

(A) Confocal images of cells incubated with G/R@TKP or G/R@TKP/HA for different time. All images share the same scale bar of 75 μm . (B) Quantitative analysis of vector fluorescence intensity in (A) ($n = 3$). ns: $P > 0.05$, $0.01 < *P < 0.05$, $0.001 < **P < 0.01$, $0.0001 < ***P < 0.001$, $0.00001 < ****P < 0.0001$, calculated with the T-test.

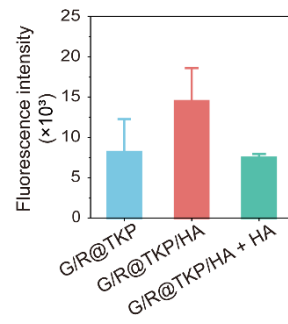


Fig. S12.

Quantitative analysis of TCM fluorescence intensity in cellular uptake experiment of G/R@TKP, G/R@TKP/HA and G/R@TKP/HA + HA.

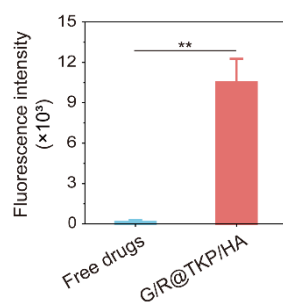


Fig. S13.

Quantitative analysis of Cy5 fluorescence intensity in cellular uptake experiment of Free drugs (Gem + $Cy5$ siRNA) and G/R@TKP/HA ($n = 3$). ns: $P > 0.05$, $0.01 < *P < 0.05$, $0.001 < **P < 0.01$, $0.0001 < ***P < 0.001$, $0.00001 < ****P < 0.0001$, calculated with the T-test.

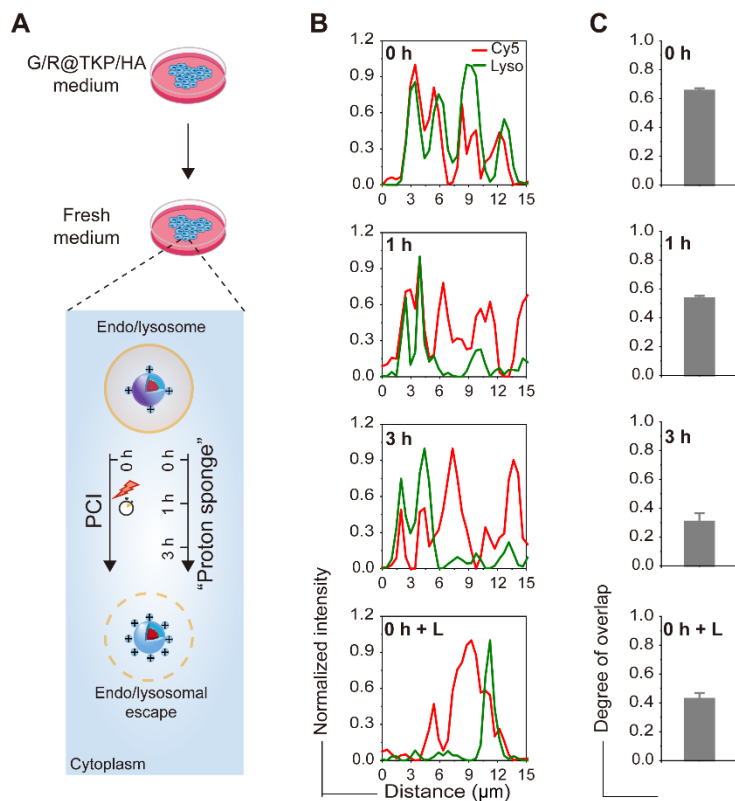


Fig. S14.

(A) Schematic illustration of endo/lysosomal escape approach of G/R@TKP/HA. (B) Overlapping profiles of Cy5 and LysoTracker Red fluorescent signals along the selected line across the cell (indicated by a red line in the zoomed-in image in Fig. 3G). (C) Pearson's correlation coefficients of Cy5 and LysoTracker Red along the selected line across the cell (indicated by a red line in the zoomed-in image in Fig. 3G).

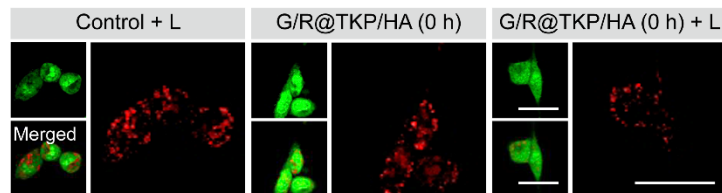


Fig. S15.

Lysosomal membrane damage of G/R@TKP/HA induced by ROS using acridine orange (AO) as the indicator. After 1 h incubation with G/R@TKP/HA, G/R@TKP/HA medium was replaced. For the light group, the cells were exposed to white light (40 mW cm^{-2} , 8 min) before AO staining. AO exhibits green fluorescence within cytoplasm and nuclei, while emitting red fluorescence in endo/lysosomes. All images share the same scale bar of $25 \mu\text{m}$.

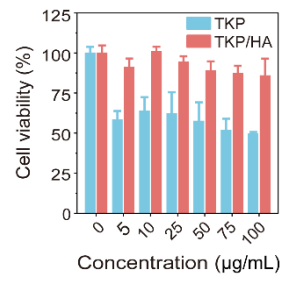


Fig. S16.
Cell viability after incubated with TKP or TKP/HA at different concentrations.

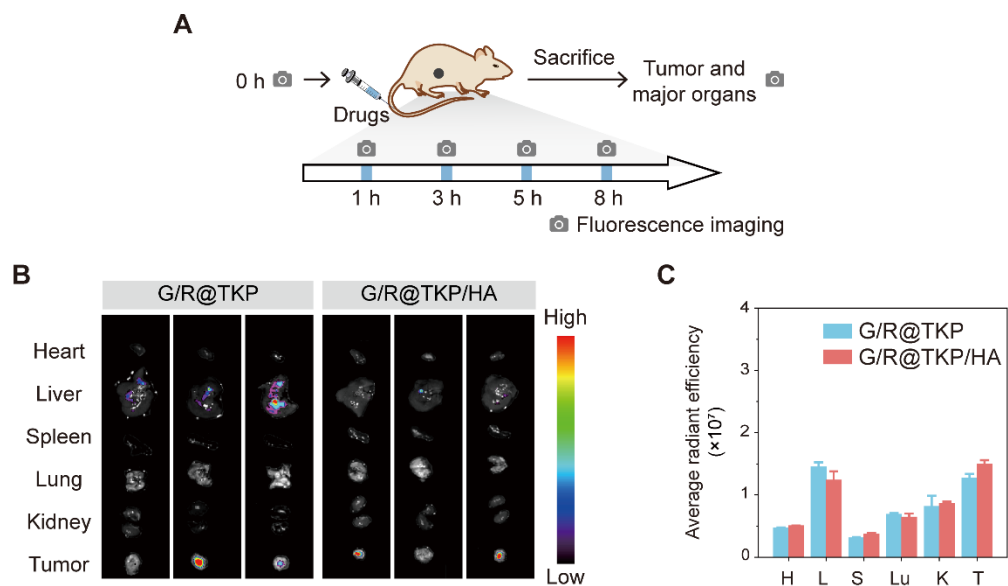


Fig. S17.

(A) Schematic illustration of *in vivo* fluorescence imaging process for the PANC1 tumor bearing mice. (B) *Ex vivo* fluorescent images of major organs and tumors from PANC1 tumor bearing mice injected intravenously with G/R@TKP or G/R@TKP/HA at 8 h ($n = 3$). (C) Quantitative analysis of fluorescence intensity in (B). H: heart; L: liver; S: spleen; Lu: lung; K: kidney; T: tumor.

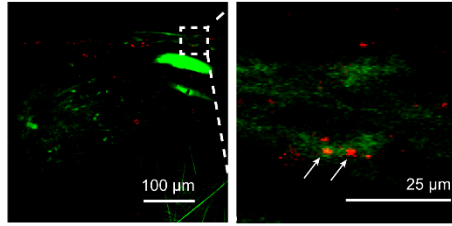


Fig. S18.

Confocal imaging of tumor region of PANC1 tumor bearing mice injected intravenously with G/R@TKP/HA ($n = 1$). Vessels stained with Evans Blue are shown in green.

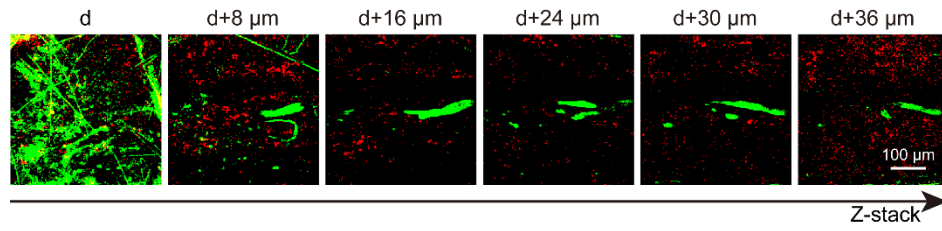


Fig. S19.

Confocal imaging of tumor region along the z-axis at different depths of PANC1 tumor bearing mice injected intravenously with G/R@TKP/HA ($n = 1$). Vessels stained with Evans Blue are shown in green.

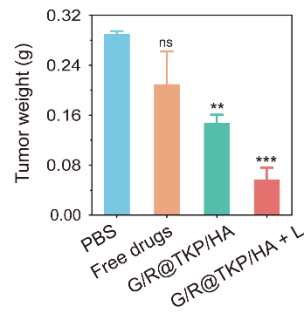


Fig. S20.

Tumor weights of different groups at the end of treatment ($n = 4$). ns: $P > 0.05$, $0.01 < *P < 0.05$, $0.001 < **P < 0.01$, $0.0001 < ***P < 0.001$, $0.00001 < ****P < 0.0001$, calculated with the T-test.

3 Characterization of Compounds

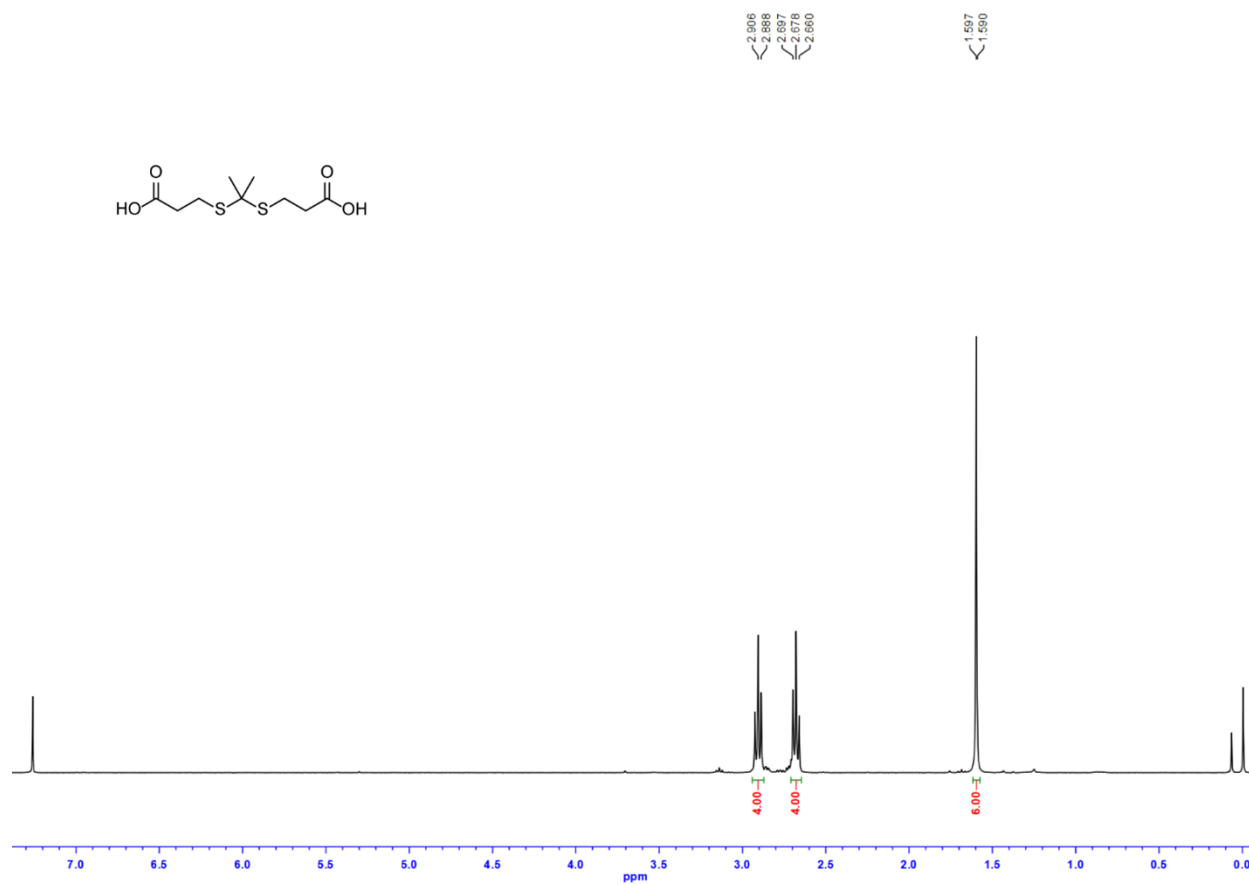
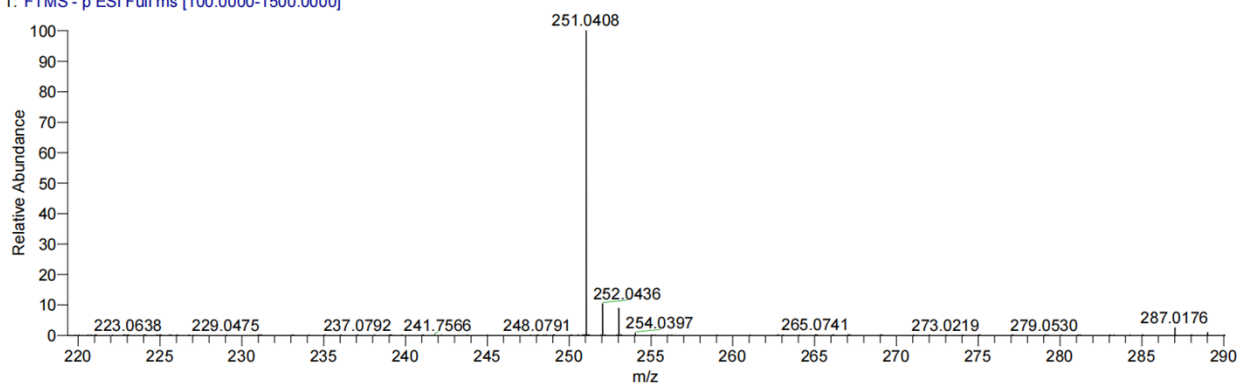


Fig. S21.

¹H NMR spectrum of TK-COOH in CDCl₃.

ZW-SYQ-1#1-42 RT: 0.01-0.22 AV: 42 NL: 8.25E8
T: FTMS - p ESI Full ms [100.0000-1500.0000]



ZW-SYQ-1#1-42 RT: 0.01-0.22 AV: 42
T: FTMS - p ESI Full ms [100.0000-1500.0000]
m/z = 250.82-251.23

m/z	Intensity	Relative	Theo. Mass	Delta (ppm)	Composition
251.0408	841878144.0	100.00	251.0406	0.18	C ₉ H ₁₅ O ₄ S ₂

Fig. S22.

HRMS spectrum of TK-COOH.

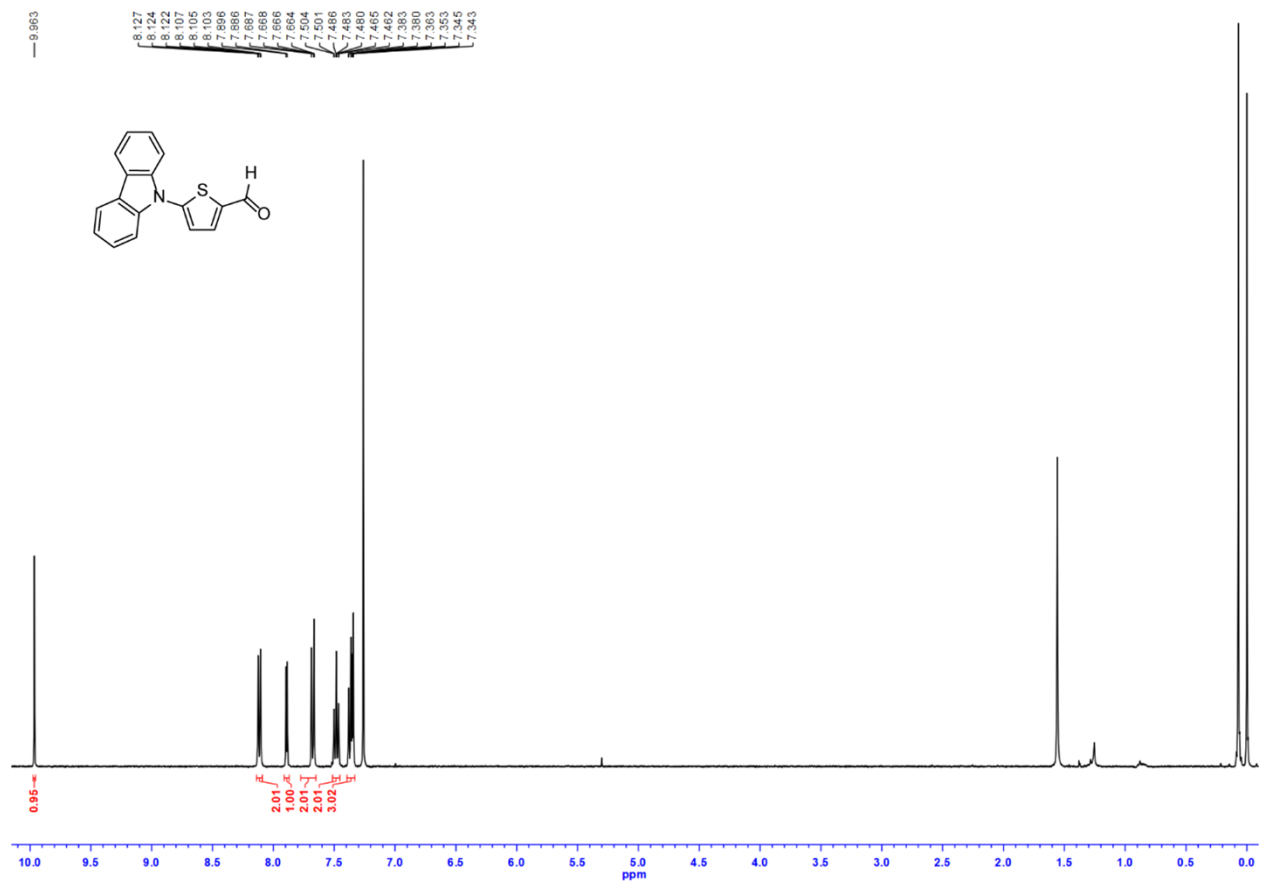
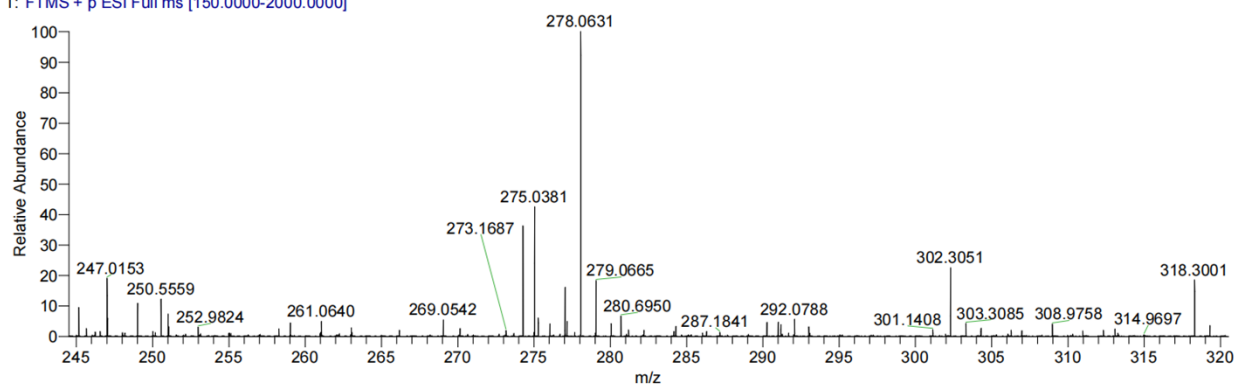


Fig. S23.
¹H NMR spectrum of Cz-T-CHO in CDCl₃.

ZW-SYQ-2#1-71 RT: 0.00-0.36 AV: 71 NL: 1.29E8
T: FTMS + p ESI Full ms [150.0000-2000.0000]



ZW-SYQ-2#1-71 RT: 0.00-0.36 AV: 71
T: FTMS + p ESI Full ms [150.0000-2000.0000]
m/z = 277.69-278.43

m/z	Intensity	Relative	Theo. Mass	Delta (ppm)	Composition
278.0631	130791224.0	100.00	278.0634	-0.28	C ₁₇ H ₁₂ O ₂ N ₂ S

Fig. S24.

HRMS spectrum of Cz-T-CHO.

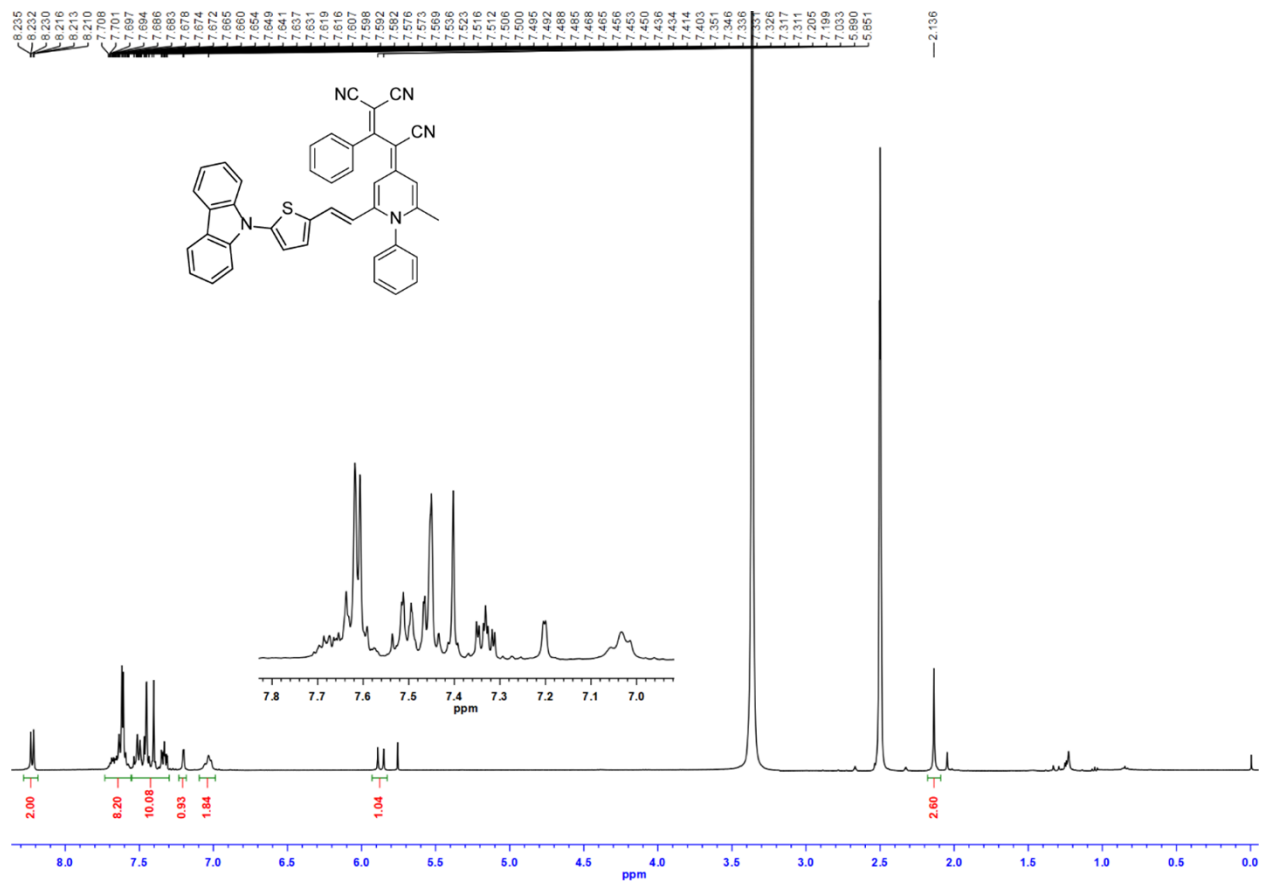
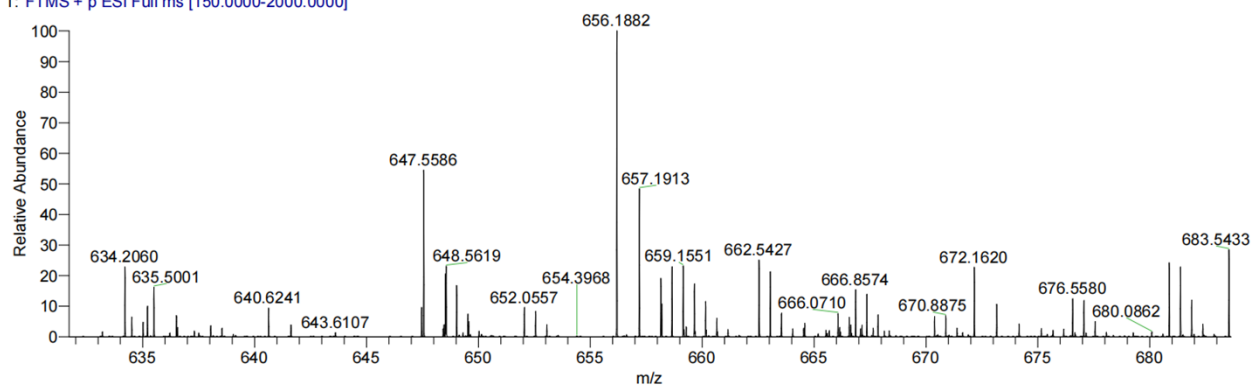


Fig. S25.

^1H NMR spectrum of TCM-Cz in $\text{DMSO-}d_6$.

ZW-SYQ-3_20240429153209#39-99 RT: 0.20-0.50 AV: 61 NL: 1.14E7
 T: FTMS + p ESI Full ms [150.0000-2000.0000]



ZW-SYQ-3_20240429153209#39-101 RT: 0.20-0.51 AV: 63

T: FTMS + p ESI Full ms [150.0000-2000.0000]

m/z = 655.82-656.49

m/z	Intensity	Relative	Theo. Mass	Delta (ppm)	Composition
656.1882	11491907.0	100.00	656.1879	0.27	C ₄₂ H ₂₇ N ₅ Na S

Fig. S26.

HRMS spectrum of TCM-Cz.

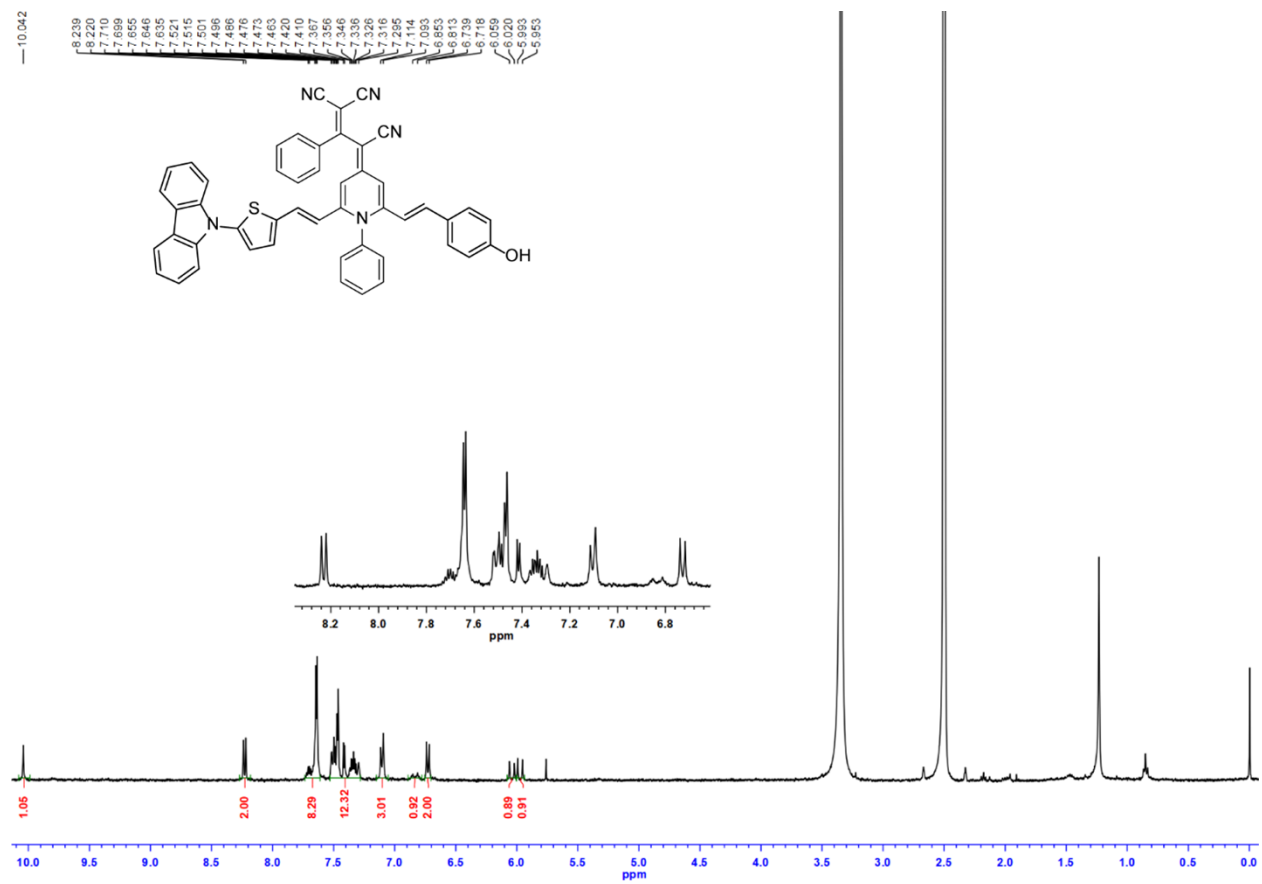
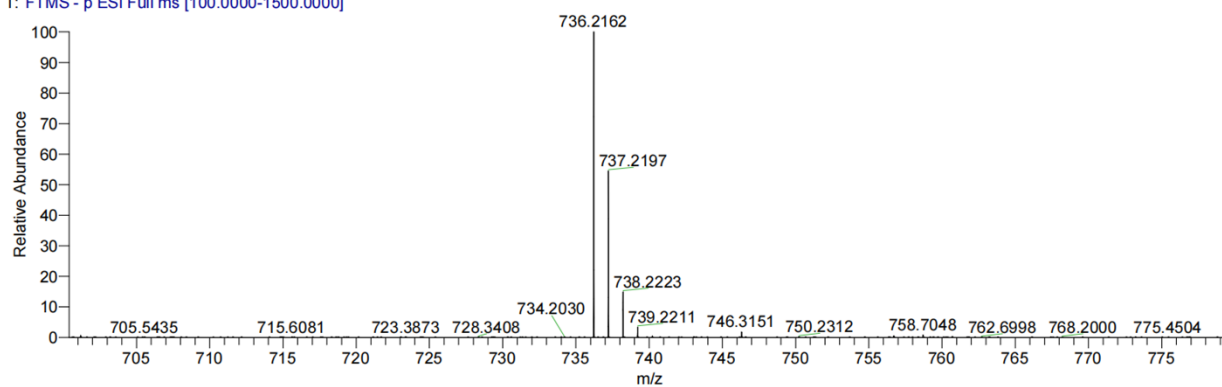


Fig. S27.
¹H NMR spectrum of TCM-Cz-OH in DMSO-*d*₆.

ZW-SYQ-4#1-191 RT: 0.01-1.00 AV: 191 NL: 5.01E6
T: FTMS - p ESI Full ms [100.0000-1500.0000]



ZW-SYQ-4#1-191 RT: 0.01-1.00 AV: 191
T: FTMS - p ESI Full ms [100.0000-1500.0000]
m/z = 735.72-736.49

m/z	Intensity	Relative	Theo. Mass	Delta (ppm)	Composition
736.2162	5041768.5	100.00	736.2166	-0.36	C ₄₉ H ₃₀ O _N ₅ S

Fig. S28.

HRMS spectrum of TCM-Cz-OH.

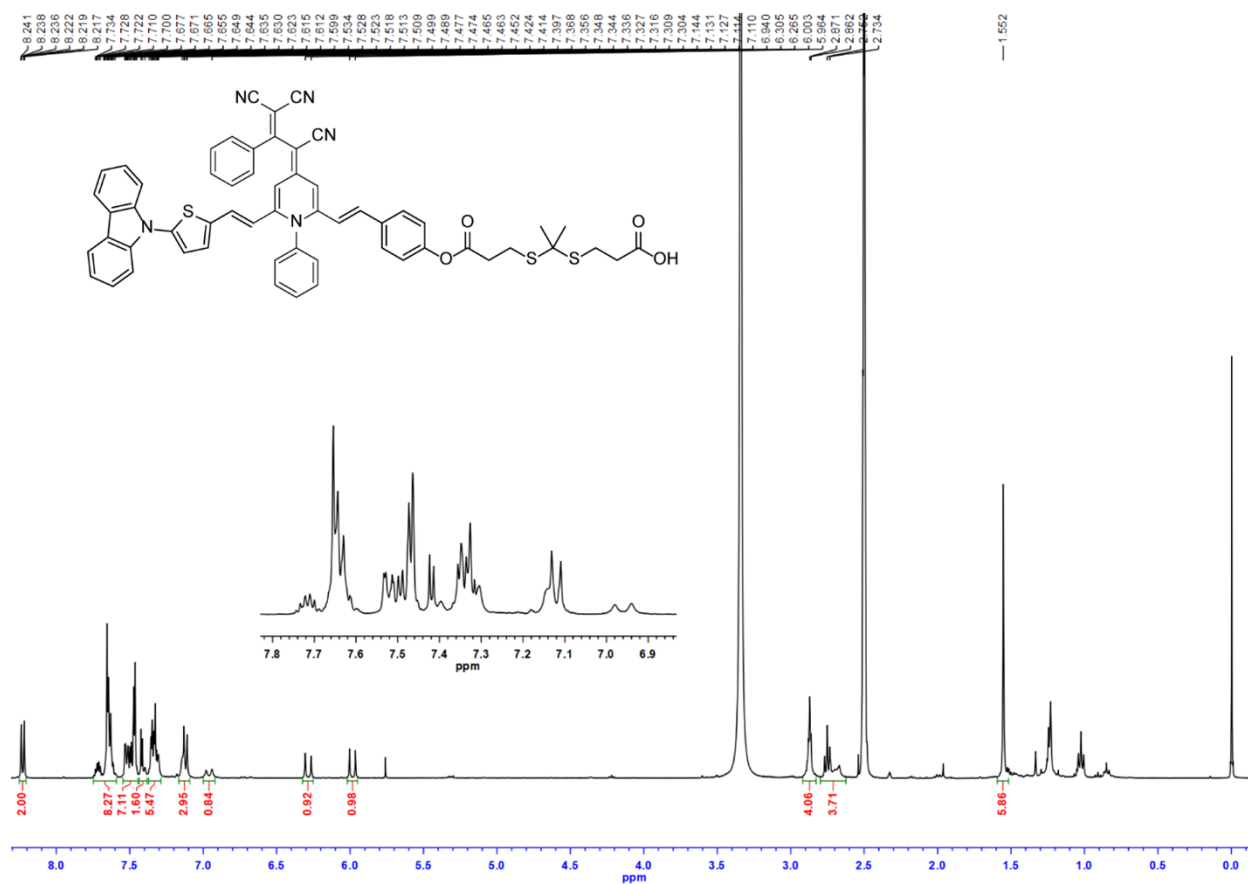


Fig. S29.

¹H NMR spectrum of TCM in DMSO-d₆.

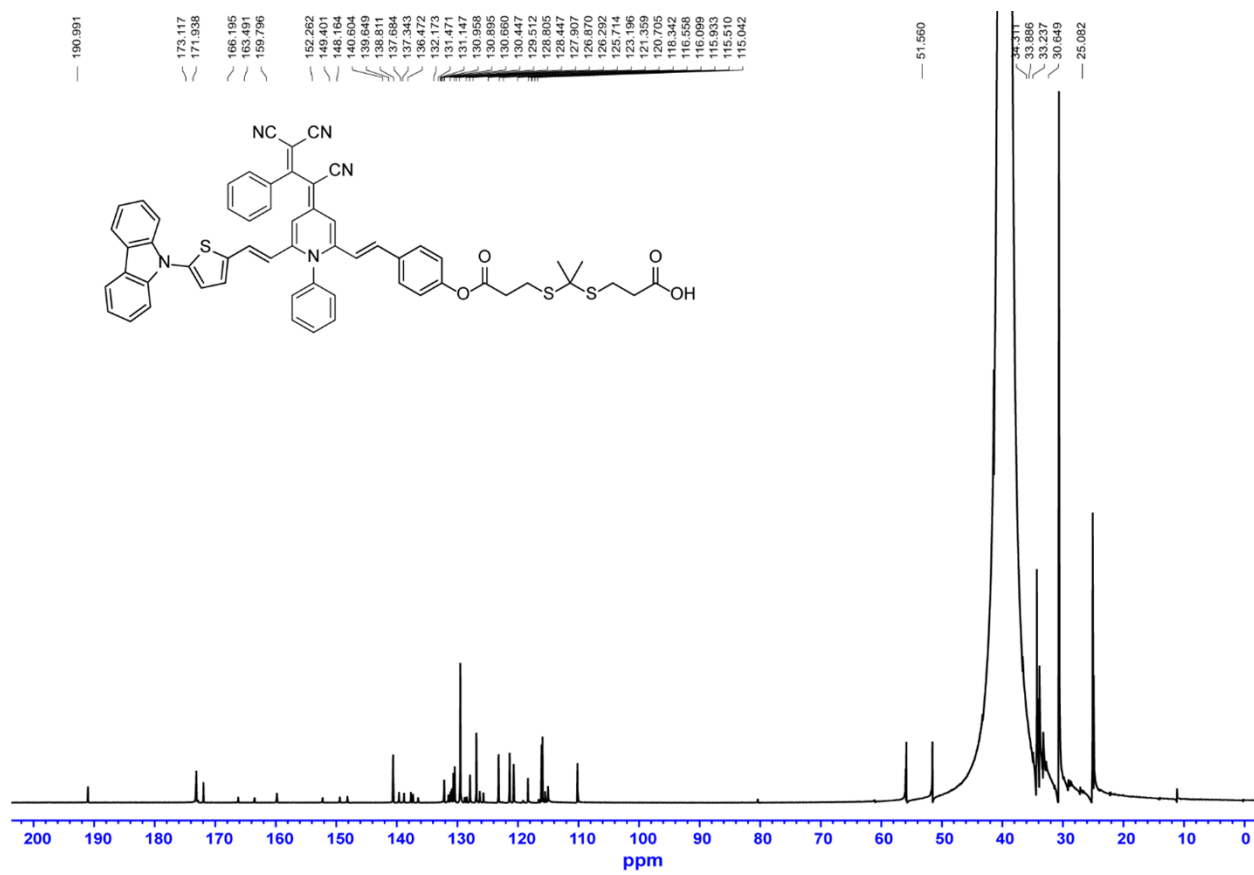
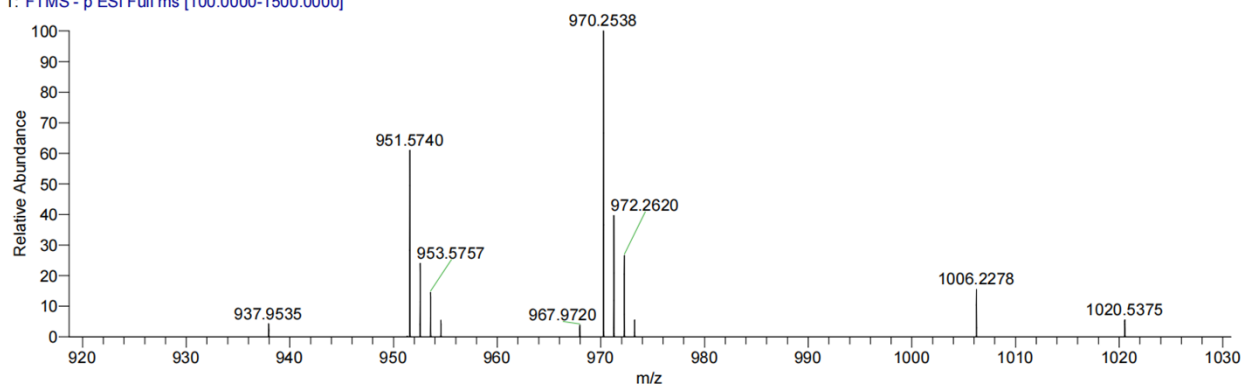


Fig. S30.

¹³C NMR spectrum of TCM in DMSO-*d*₆.

ZW-SYQ-5_20240429151054 #69-75 RT: 0.45-0.49 AV: 7 NL: 1.08E5
T: FTMS - p ESI Full ms [100.0000-1500.0000]



ZW-SYQ-5_20240429151054 #69-75 RT: 0.45-0.49 AV: 7

T: FTMS - p ESI Full ms [100.0000-1500.0000]

m/z = 970.21-970.31

m/z	Intensity	Relative	Theo. Mass	Delta (ppm)	Composition
970.2538	110996.5	100.00	970.2550	-1.20	C ₅₈ H ₄₄ O ₄ N ₅ S ₃

Fig. S31.

HRMS spectrum of TCM.

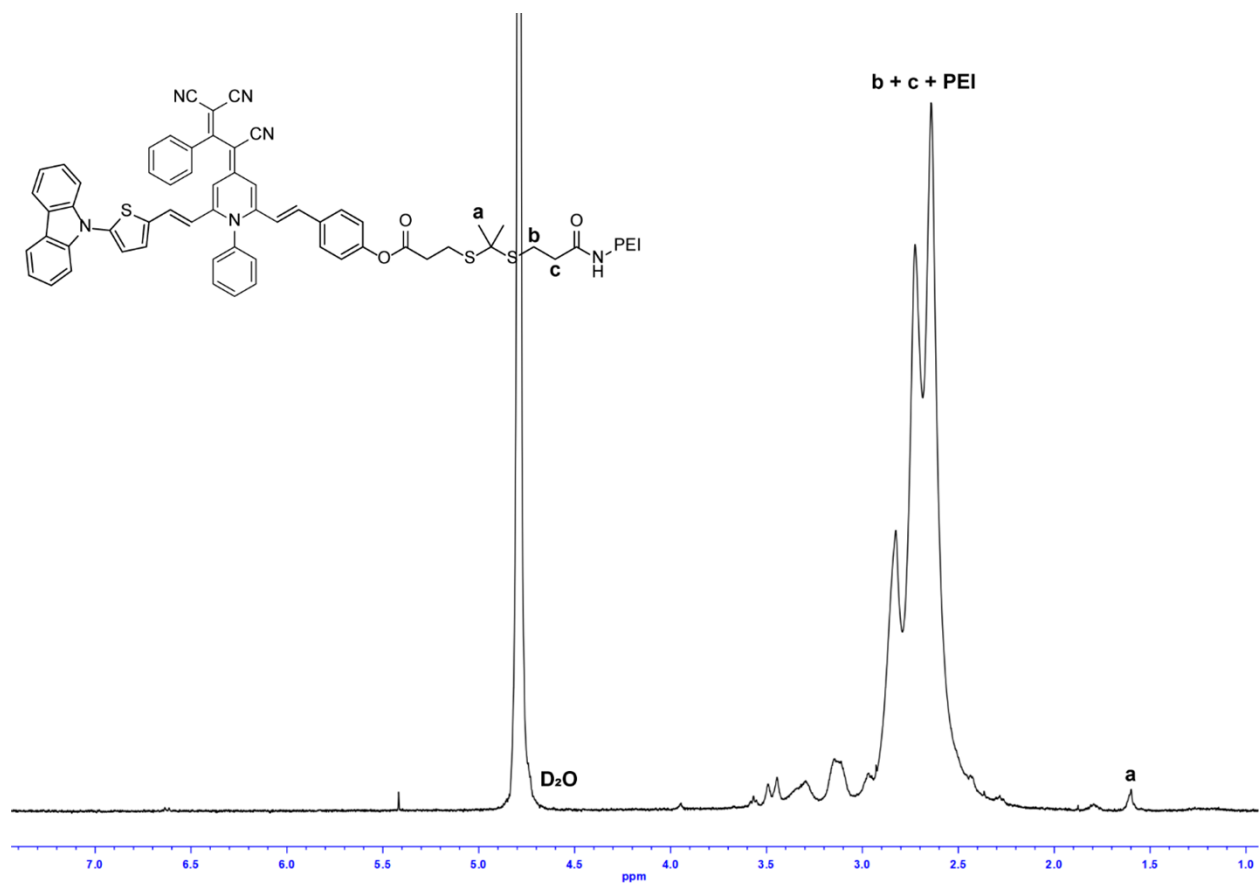


Fig. S32.

^1H NMR spectrum of TCM-TK-PEI in D_2O .

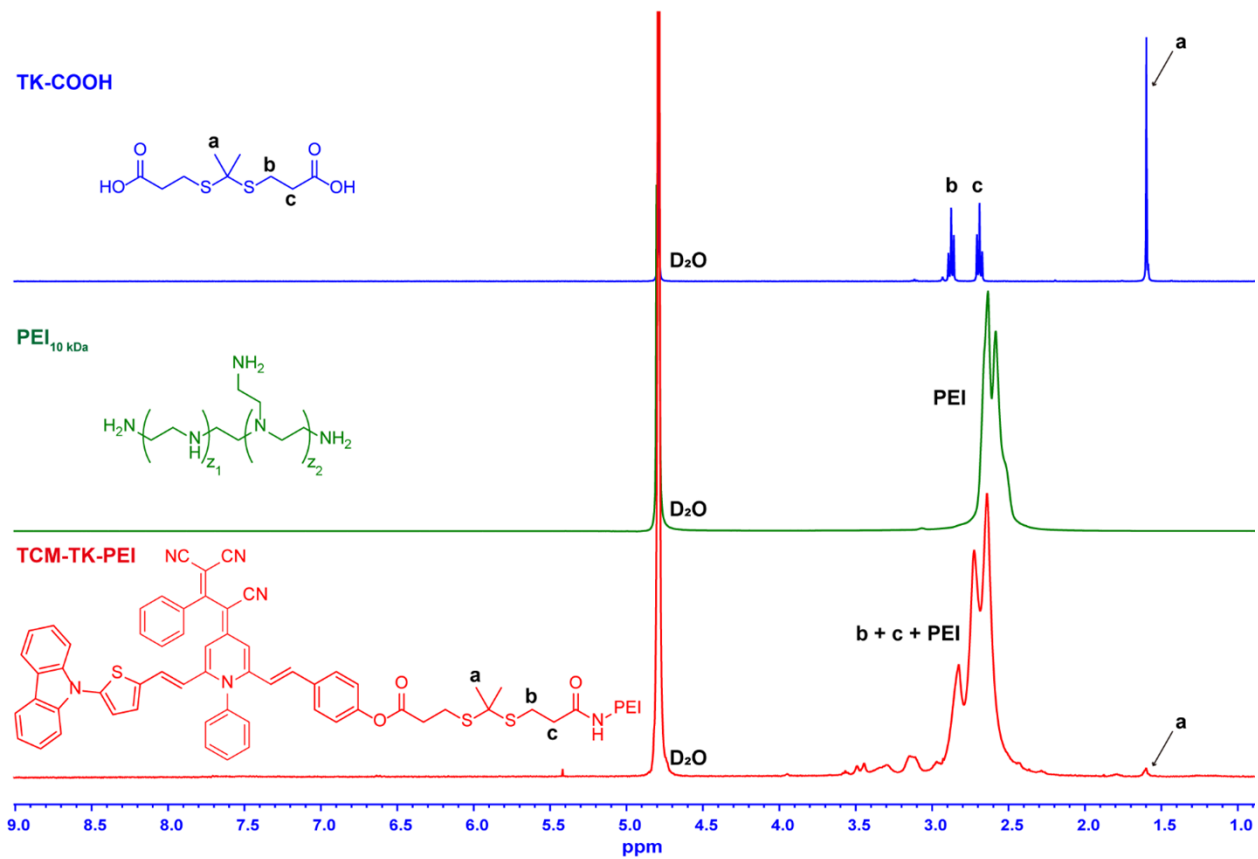
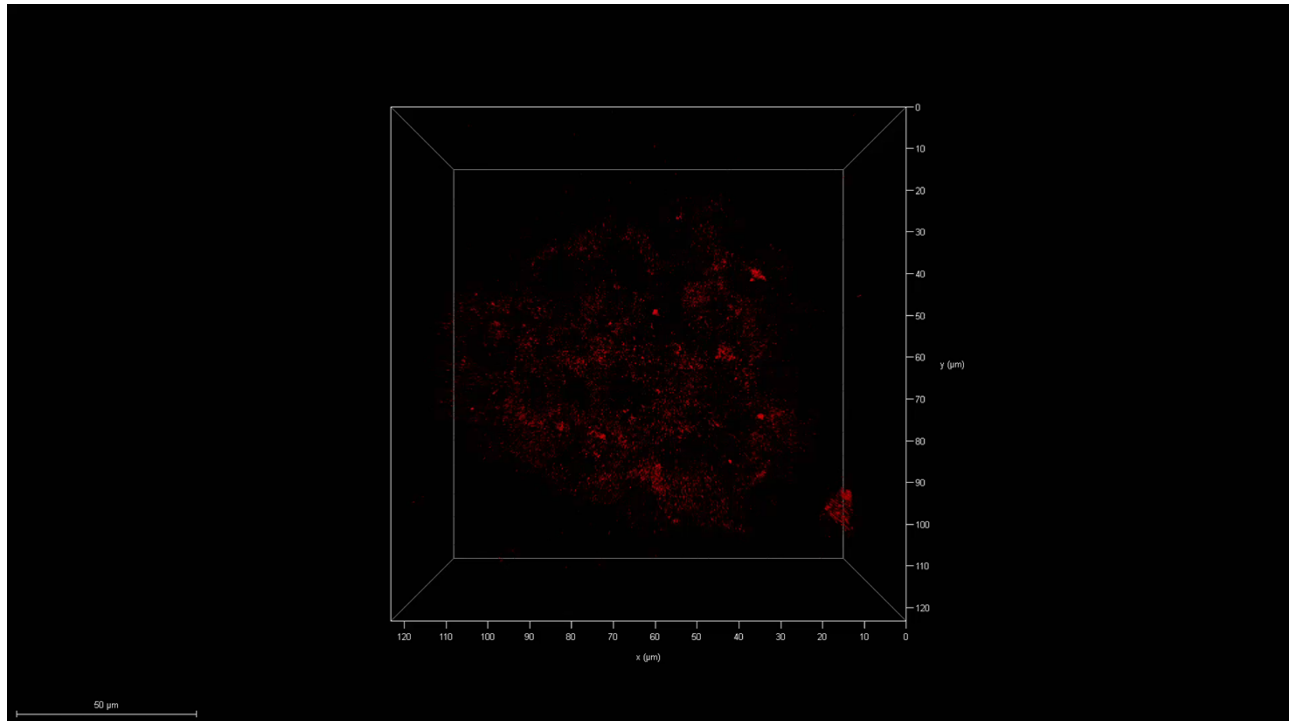


Fig. S33.

¹H NMR spectra of TK-COOH, PEI, and TCM-TK-PEI in D₂O.

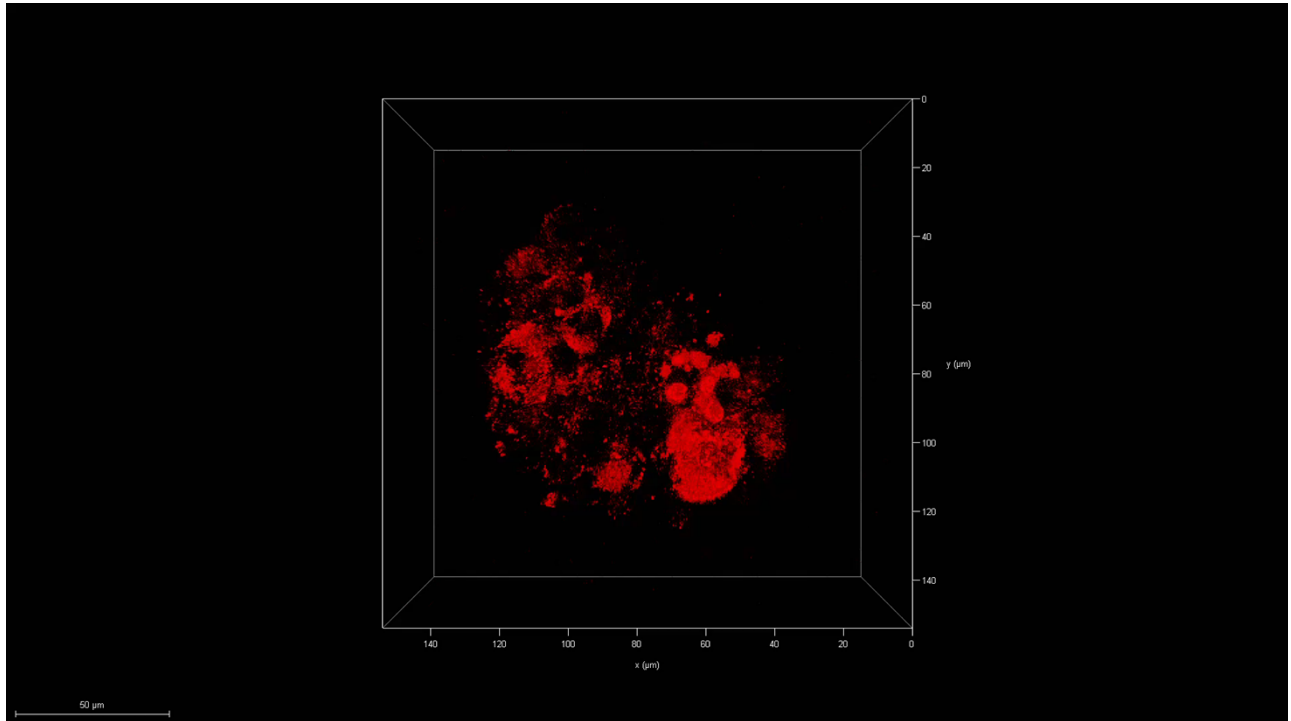
4 Supporting Movies

Movie S1.



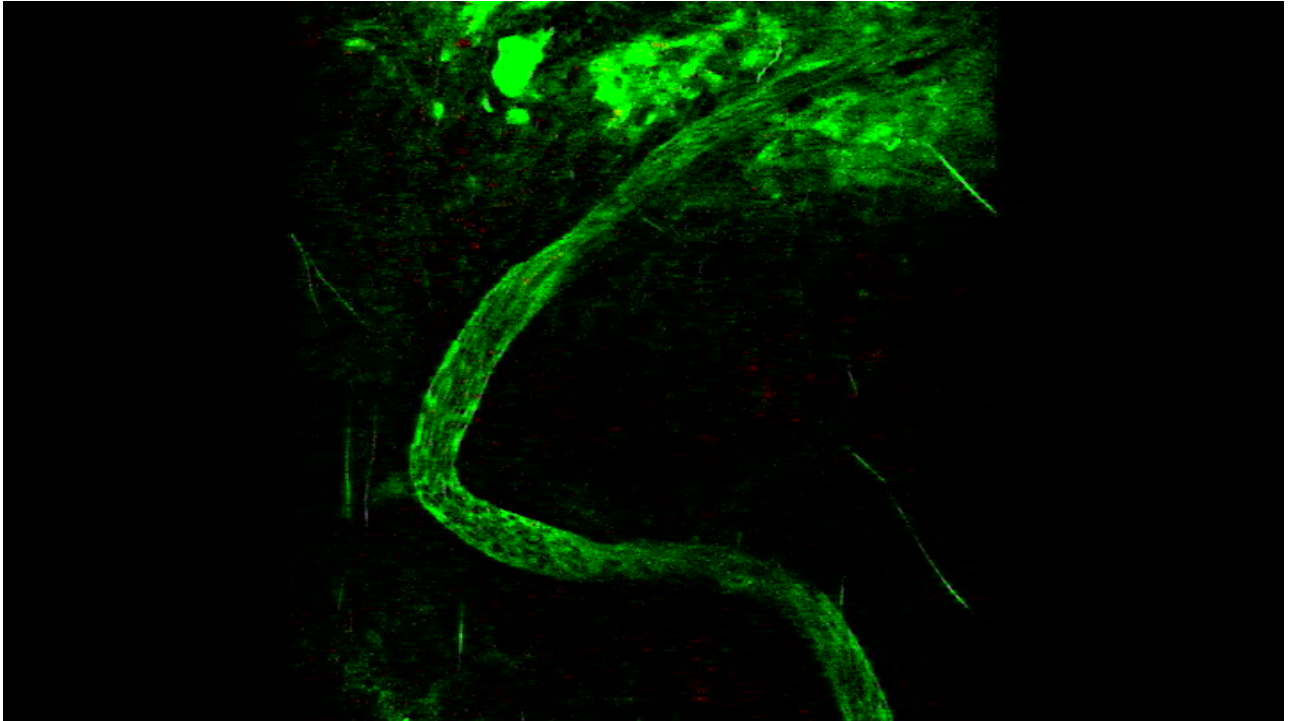
Three-dimensional reconstruction of PANC1 MTSs treating with G/R@TKP.

Movie S2.



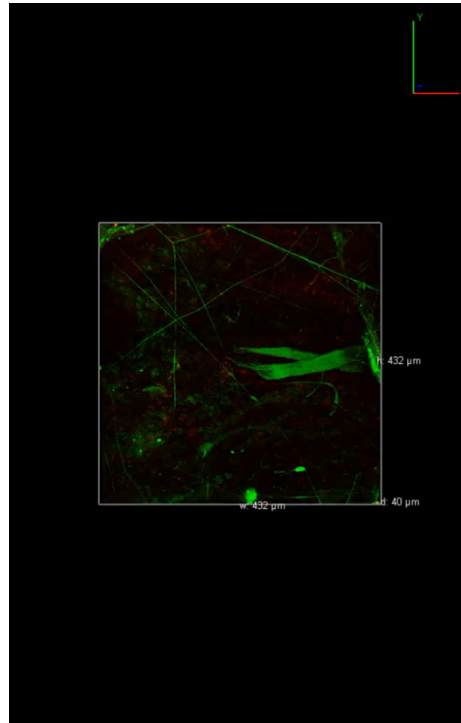
Three-dimensional reconstruction of PANC1 MTSs treating with G/R@TKP/HA.

Movie S3.



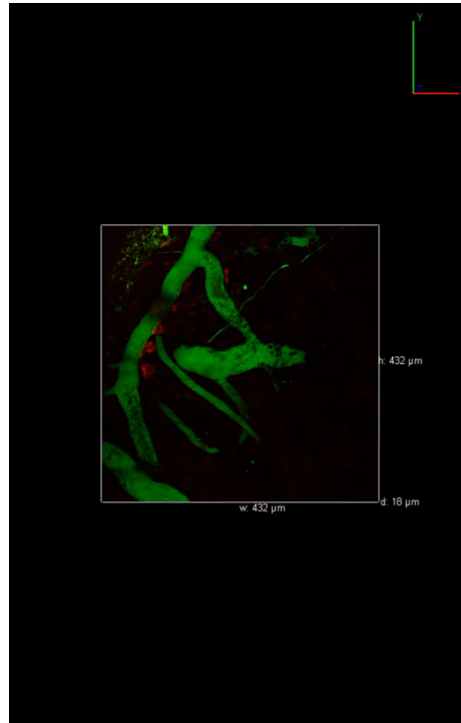
Real-time visualization of the flow of red fluorescent G/R@TKP/HA in vessels. Vessels stained with Evans Blue are shown in green.

Movie S4.



Three-dimensional reconstruction of tumor region in Fig. 5G.

Movie S5.



Three-dimensional reconstruction of tumor region in Fig. 5H.